Technical Report:

Van KIRAP Rainfall and Windspeed Projections

By Savin Chand, Soubhik Biswas and Krishneel Sharma
Centre for New Energy and Transition Research, Federation University, Mt Helen Campus, Victoria, Australia

Kevin Hennessy, Leanne Webb and Geoff Gooley
CSIRO Environment, Aspendale, Victoria, Australia

Sustainable, transformative and resilient for a Blue Pacific

SPREP Library – Cataloguing in Publication data

VanKIRAP rainfall and windspeed projections: technical report. Apia, Samoa : SPREP, 2023.

.

Page numbers 24p, Size 29cm

ISBN: 978-982-04-1229-3 (ecopy)

1. Climatic changes – Vanuatu.
2. Rain and rainfall measurements – Vanuatu.

I. Pacific Regional Environment Programme (SPREP).
II. Title.

551.60959 5

Cover photo: Sunny Kamuta Seuseu

Other photos: Unless otherwise acknowledged, all images were created by the authors and VanKIRAP Project

Designed by: www.addiestudio.com

Sustainable, transformative and resilient for a Blue Pacific

PO Box 240
Apia, Samoa
T: +685 21929
E: sprep@sprep.org
W: www.sprep.org

Our vision:

A resilient Pacific environment sustaining our livelihoods and natural heritage in harmony with our cultures.

CONTENTS:

Summary

This report provides a brief overview of the dataset and methodology used to create projection information for extreme rainfall and windspeed, as well as tropical cyclone intensity, for various locations in Vanuatu. Results for only two locations (Port Vila and Luganville) are shown as examples. Two time periods are considered (2040-2070 and 2070-2100), relative to a baseline of 1970-2000, for low (Representative Concentration Pathways, RCP4.5) and high (RCP8.5) greenhouse gas emissions scenarios, from 7-8 climate models from phase 5 of the Coupled Model Intercomparison Project (CMIP5, reader is referred to (van Vuuren et al., 2011) for details on RCP experimental designs).

For extreme daily rainfall with return periods of 10-100 years, the multi-model mean results for Port Vila showed an increase of about 21% for 2040-2070 RCP4.5, 30% for 2070-2100 RCP4.5, 40% for 2040-2070 RCP8.5 and 70% for 2070-2100 RCP8.5. For return periods of 10-100 years, the multi-model mean results for Luganville showed an increase of about 18% for 2040-2070 RCP4.5, 27% for 2070-2100 RCP4.5, 26% for 2040-2070 RCP8.5 and 57% for 2070-2100 RCP8.5. These increases have significant implications for future flood risk management strategies.

For extreme daily windspeed with return periods of 10-100 years, the multi-model mean results showed an increase in intensity of about 6% for Port Vila and 3% for Luganville by 2070-2100 for RCP8.5. These increases have implications for future cyclone risk management strategies.

Introduction

Vanuatu is highly exposed to climate variability and change. The Green Climate Fund is supporting the Van KIRAP Project which is delivering climate information services (CIS) to inform decision-making by sectors and communities in Vanuatu. This project is led by SPREP (Secretariat of the Pacific Regional Environmental Program) in partnership with VMGD (Vanuatu Meteorology & Geo-hazards Department) and delivery partners including Australia's CSIRO (Commonwealth Scientific and Industrial Research Organisation) and Federation University, along with the APEC (Asia-Pacific Economic Co-operation) Climate Centre.

More specifically, Van KIRAP will develop and demonstrate application of CIS in five priority sectors: infrastructure, water, agriculture, fisheries and tourism. Sectoral case studies will include hazard-based climate change impact assessments for each of the sectors to facilitate development and demonstration of the application of CIS at multi-decadal timescales.

Van KIRAP will build the technical capacity of key sectoral stakeholders to use CIS including climate data, information, tools and other science-based resources. The project will support enhanced coordination and dissemination of CIS products and services to inform climate change impact/risk assessments and associated adaptation planning at sectoral level.

The water and infrastructure sectors require information about current and future extreme rainfall and wind. This technical report describes data and methods used to estimate extreme rainfall and windspeed intensity and frequency for Vanuatu. It is anticipated that the approach described in this report can be adopted for other countries in the Pacific, and elsewhere around the globe.

1. Rainfall and windspeed data and calibrations

Daily rainfall data

For the current and future projections of daily rainfall, this report uses station data, ERA5 reanalysis data and rainfall data from Coupled Climate Model Intercomparison Project phase 5 (CMIP5) climate models (Taylor et al., 2012).

Historical emissions, medium future emissions (RCP 4.5) and high future emissions (RCP 8.5) scenarios (Moss et al., 2010) were used for the seven CMIP5 models in the study (Table 1). These models were selected because (a) they perform well in simulating the current climate and (b) they represent a broad range of future climates.

Table 1: List of CMIP5 Models used for rainfall

CMIP5 MODELS	HISTORICAL PERIOD	RCP8.5 PERIOD	RCP4.5 PERIOD
ACCESS1.0	1850-2005	2006-2100	2006-2100
CanESM2	1850-2005	2006-2100	2006-2100
GFDL-ESM2M	1850-2005	2006-2100	2006-2100
GISS-E2-H	1850-2005	2006-2100	2006-2100
IPSL-CM5A-LR	1850-2005	2006-2100	2006-2300
IPSL-CM5A-MR	1850-2005	2006-2100	2006-2100
NorESM1-M	1850-2005	2006-2100	2006-2300

Since the above CMIP5 models had coarse spatial resolution (about 200 km between data points) and contain systematic biases, the output data need to be calibrated. This can be done using geospatial interpolation (Li and Heap, 2014) and bias correction (Piani et al., 2010). The following three steps were carried out to calibrate the above-mentioned CMIP5 models.

1. Fill in missing values in weather station data
2. Calibrate ERA5 reanalysis data on a 30 km grid using weather station data
3. Interpolate and bias-correct the climate model data using the calibrated ERA5 data

Step 1

Temporal homogeneity was ensured for daily rainfall data obtained from seven VMGD weather stations (see Table 2 and Figure 1) across Vanuatu by filling in missing values using the Inverse distance weighting (IDW) interpolation technique. IDW was chosen for its simplicity and low computation load (Li and Heap, 2014).

Table 2: List of VMGD weather stations

STATION NAME	LATITUDE (OE)	LONGITUDE (OS)
Sola	167.55	13.85
Pekoa	167.22	15.52
Lamap	167.8	16.42
Bauerfield	168.3	17.7
Port Vila	168.32	17.74
White Grass	169.22	19.45
Aneityum	169.77	20.23

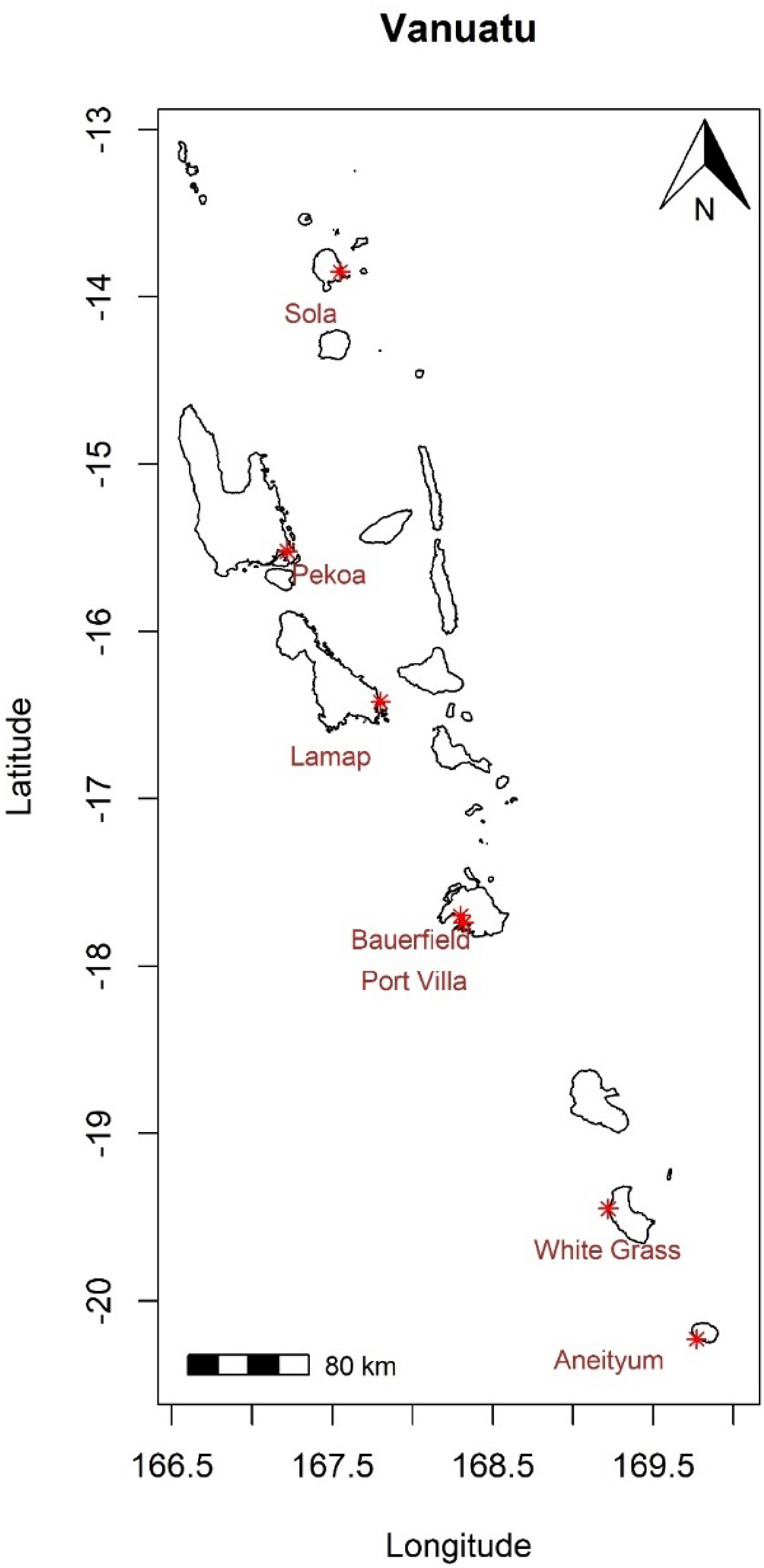

Figure 1: Map of Vanuatu showing the locations of VMGD weather stations.

Step 2

The ERA5 reanalysis dataset is available on a 30 km grid from 1940-2022. The daily accumulated rainfall for ERA5 is calculated from hourly ERA5 rainfall after accounting for the local time zone conversion from the UTC. The ERA5 daily accumulated rainfall data were then calibrated with the VMGD weather station data nearest to each grid point. This was done using quantile-quantile matching (bin size of 450) with the help of a cubic spline approach; this approach does not assume linearity and is more appropriate for calibration of extremes (Biswas et al., 2022). Note here that the 1961 – 2005 data were used as the training period to calibrate the ERA5 daily accumulated rainfall from weather station daily rainfall data (Table 3).

Table 3: Table 3. ERA5 and station data for rainfall

DATA	STATION DATA	ERA5	CALIBRATED ERA5
Spatial Resolution	NA	0.25° X 0.25°	0.25° X 0.25°
Temporal Resolution	Daily	Hourly	Daily
Time period	1961 – Present	1960 – Present	1961 – 2005

Step 3

The CMIP5 model data were then bilinearly interpolated to the spatial resolution of calibrated ERA5 data. The bilinear interpolation technique was selected, after comparing several other methods, due to its simplicity and being computationally inexpensive (Petrou and Petrou, 2010; Wolf et al., 2014). Though other approaches might offer better accuracy while performing the geospatial interpolation, it does not matter that much in this case, as we would again need to bias-correct the CMIP5 climatic models with respect to bias-corrected ERA5 data.

The interpolated CMIP5 data were then bias-corrected using calibrated ERA5 data. It is to be noted that the daily data from CanESM2, GFDL-ESM2M, GISS-E2-H, IPSL-CM5A-MR, IPSL-CM5A-MR and NorESM1-M have no leap year (i.e., all years are 365 days in length).

In Figure 2, we have compared kernel density plots (Silverman, 1986; Sheather and Jones, 1991) of the Port Vila station-based data, uncorrected ERA5, calibrated ERA5, uncorrected CMIP5 and bias-corrected CMIP5 yearly rainfall data for each of the CMIP5 models. Visually, the calibration of ERA5 and the bias correction of CMIP5 models look promising with respect to station-based rainfall data (Figure 2). For a better comparison between each of the rainfall datasets, yearly maximum rainfall was analysed (Figure 2). This comparison was repeated for the six other locations in Table 1, and we observed a similarity between the station data, the calibrated ERA5 data and the bias-corrected CMIP5 rainfall datasets.

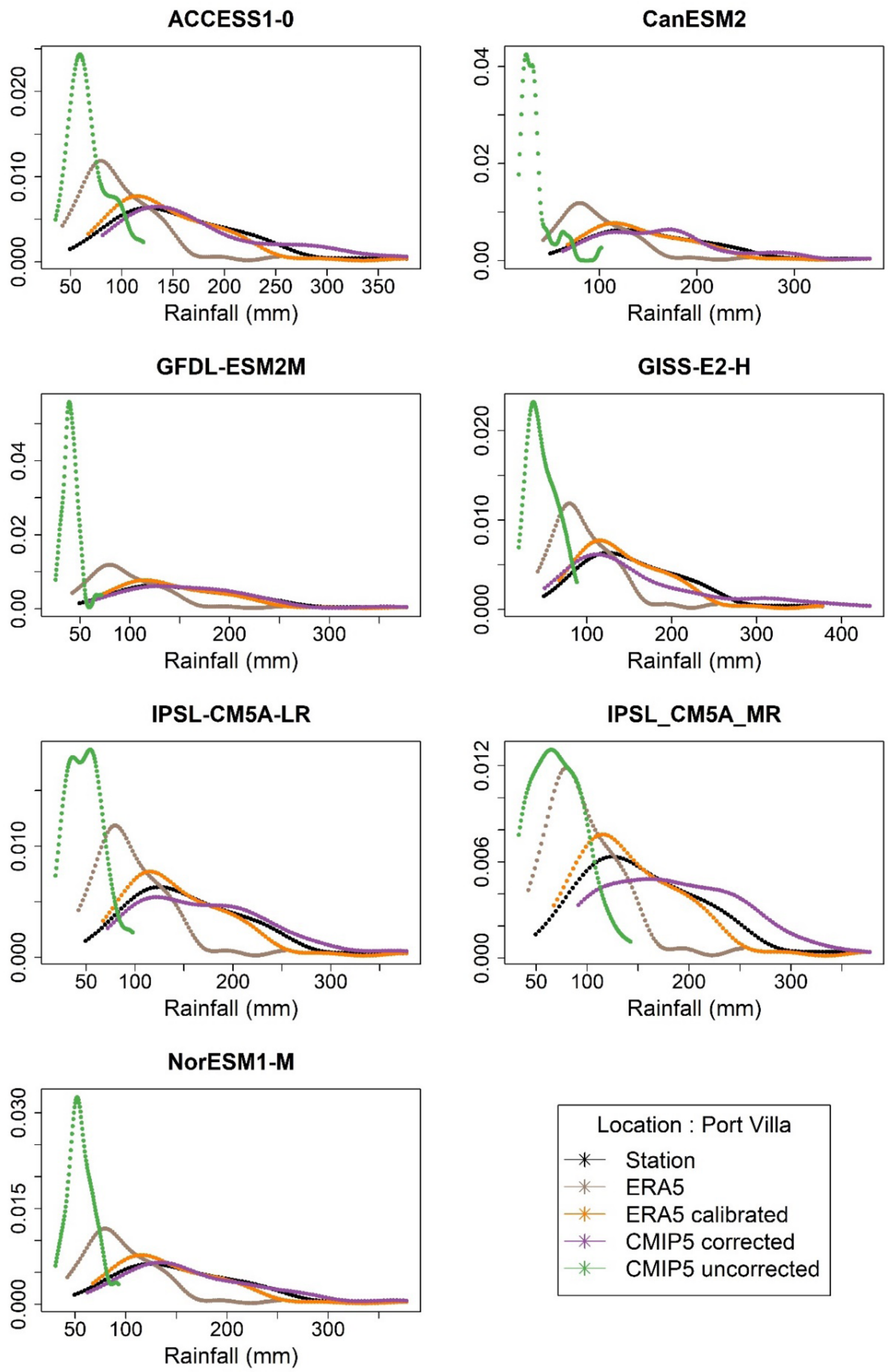

Figure 2: Comparison of kernel density graphs of daily rainfall data from 1961 to 2005 at Port Vila (168.32 E, 17.74 S) for the weather station data (black), raw ERA5 data (brown), calibrated ERA5 data (orange), uncorrected CMIP5 data (violet) and bias-corrected CMIP5 rainfall data (green). A close match between the black, orange and purple curves indicates that calibration of ERA5 data and bias-correction of CMIP5 data are performing well.

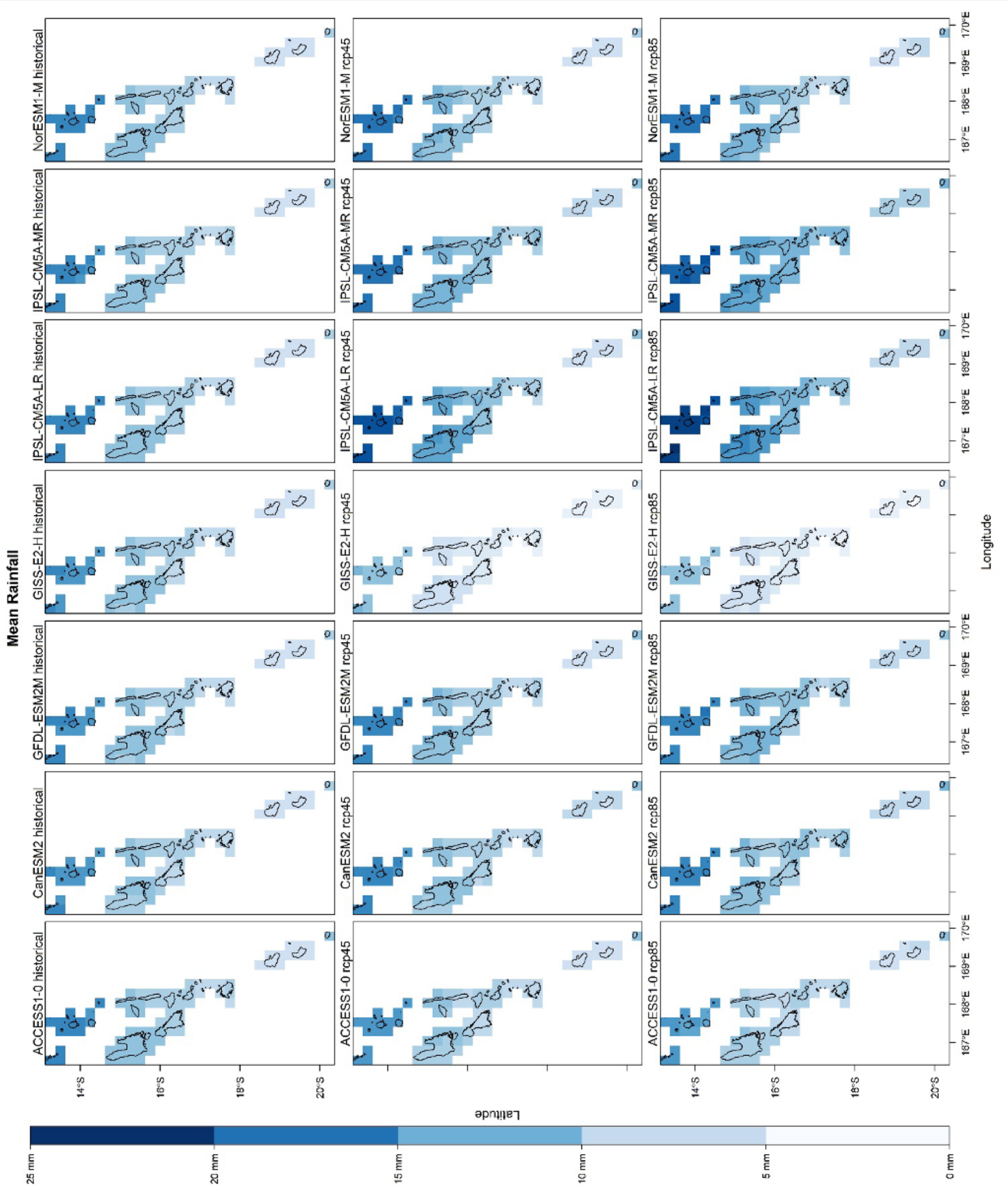

Figure 3: Climatological average daily rainfall for historical (1961 - 2005), RCP4.5 (2006 - 2100) and RCP8.5 (2006 - 2100) simulations from bias-corrected CMIP5 Models.

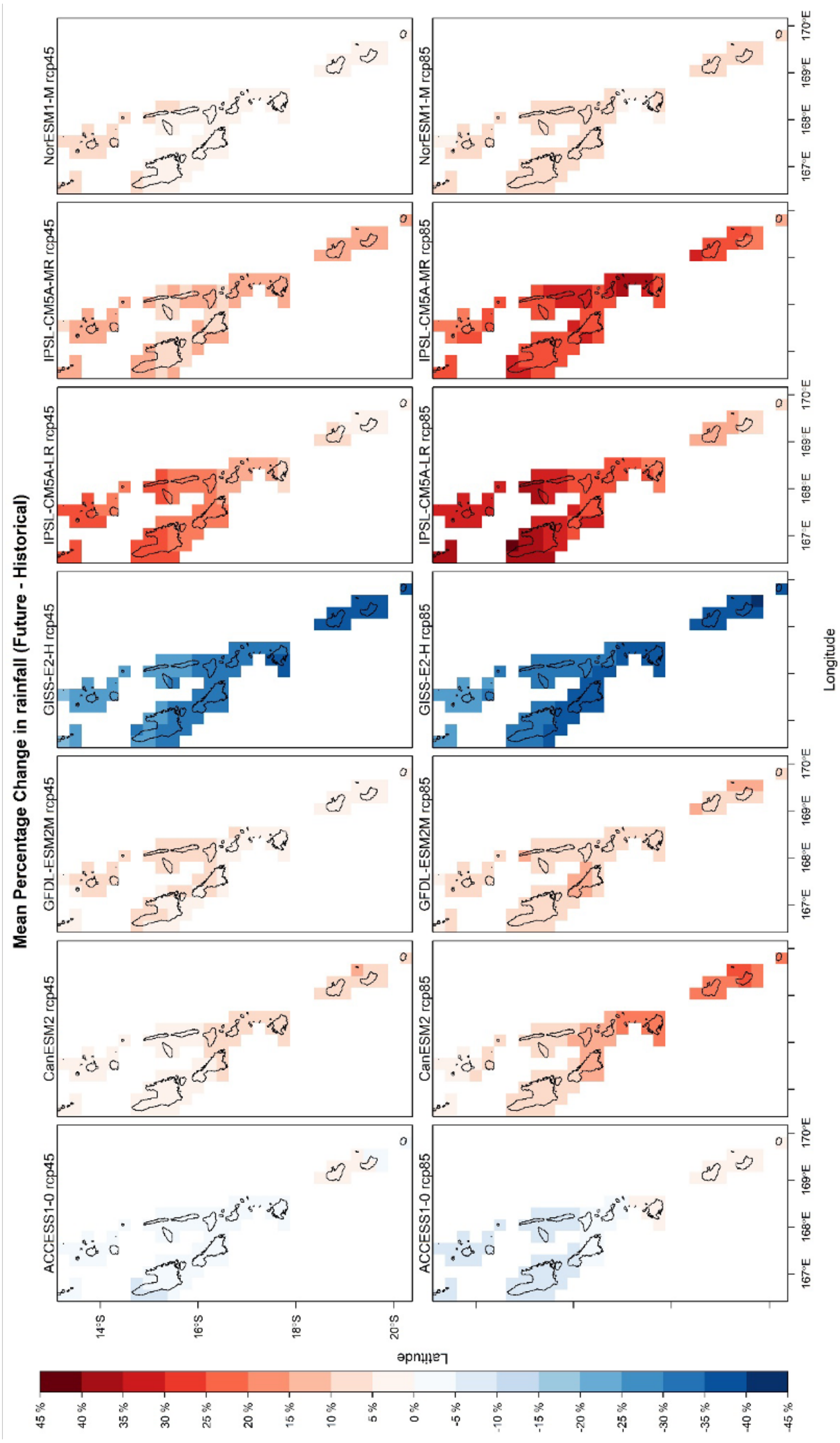

Figure 4: Mean percentage change in daily rainfall between historical (1961 – 2005) and future (2006 - 2100) simulations from bias-corrected CMIP5 Models.

To examine the bias-corrected historical, RCP4.5 and RCP8.5 CMIP5 rainfall dataset, we have calculated the climatological means for 1961 – 2005, 2006 – 2100 RCP4.5 and 2006 – 2100 RCP8.5, respectively, over Vanuatu (Figure 3). Percentage changes in daily rainfall between historical and future scenarios have also been calculated (Figure 4). Mean daily rainfall decreases in 5 of the 7 models. As the bias-corrected CMIP5 model dataset was based on the calibrated ERA5 dataset, the patterns persisted in the CMIP5 rainfall dataset as well.

Extreme value analysis of rainfall

For extreme value analysis, we selected the two locations, Luganville, Espiritu Santo (167.22 E, 15.52 S) and Port Vila, Efate (168.32 E, 17.74 S), as examples. First, the daily bias corrected CMIP5 rainfall values were extracted for these two locations (see Figure 5) and then the annual maximum daily rainfall was computed.

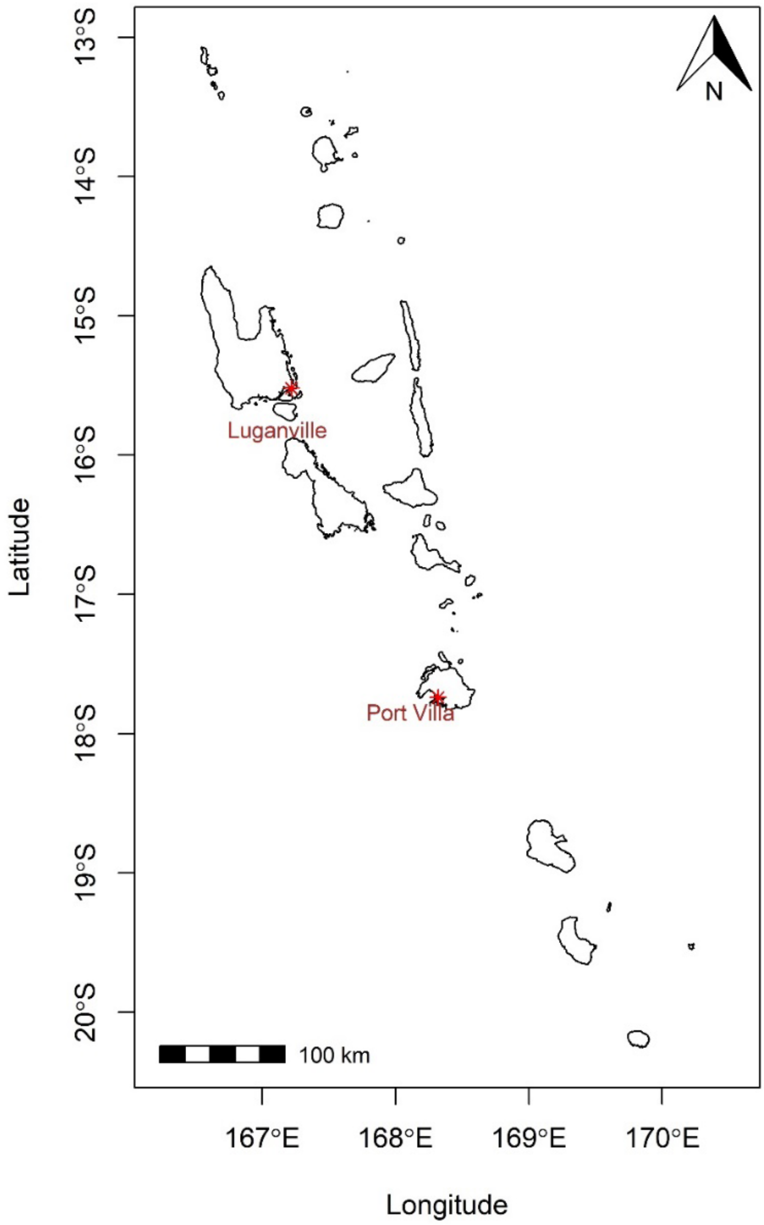

Figure 5: Map of Vanuatu showing the two locations, Luganville (167.22 E, 15.52 S) and Port Vila (168.32 E, 17.74 S).

We then computed the average recurrence interval (ARI) for various return periods. Three different periods (see Table 4) were used to compute the ARI values for 10-, 50- and 100-year return periods.

Table 4: Table 4. Baseline periods for various CMIP5 scenarios

BASELINE PERIOD	HISTORICAL	RCP8.5	RCP4.5
1970 – 2000	X		
2040 – 2070		X	X
2070 – 2100		X	X

The Gumbel distribution was used for fitting the ARI curves (Figures 6 and 7). A previous study found the Gumbel distribution to be a very good fit for ARI curves (Mudashiru et al., 2023). Results are shown for each of the seven CMIP5 models, as well as the multi-model average (Doblas-Reyes et al., 2003; Donat et al., 2010).

The multi-model results for Port Vila and Luganville indicate a general increase in extreme rainfall intensity for a given return period, with larger increases for RCP8.5 than RCP4.5, and larger increases for 2070-2100 than 2040-2070. There is some variability between the individual climate model projections for extreme rainfall, so the projections should be treated with caution. For all return periods, the multi-model mean results for Port Vila show an increase of about 21% for 2040-2070 RCP4.5, 30% for 2070-2100 RCP4.5, 40% for 2040-2070 RCP8.5 and 70% for 2070-2100 RCP8.5. For all return periods, the multi-model mean results for Luganville show an increase of about 18% for 2040-2070 RCP4.5, 27% for 2070-2100 RCP4.5, 26% for 2040-2070 RCP8.5 and 57% for 2070-2100 RCP8.5.

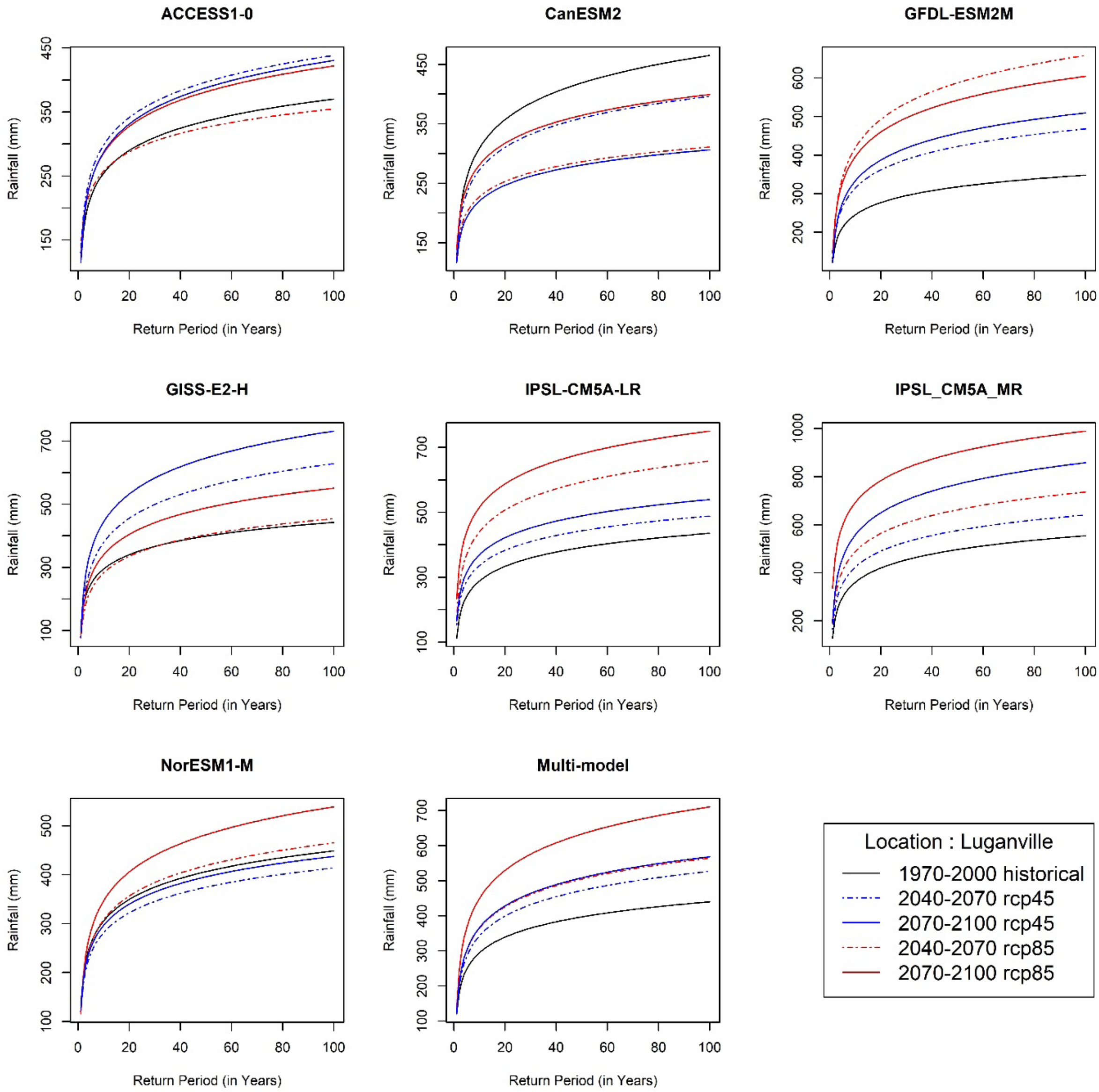

Figure 6: Average recurrence interval (ARI) curves of yearly maximum rainfall for Luganville (167.22 E, 15.52 S) using the Gumbel extreme value distribution. Comparison with historical 1970 – 2000 (black), RCP 4.5 2040 – 2070 (blue dashed) RCP 4.5 2070 – 2100 (blue), RCP 8.5 2040 – 2070 (red dashed) and RCP 8.5 2070 -2100 (red) has been shown for seven climate models and the multi-model average. The multi-model mean indicates an increase in extreme rainfall intensity for a given return period.

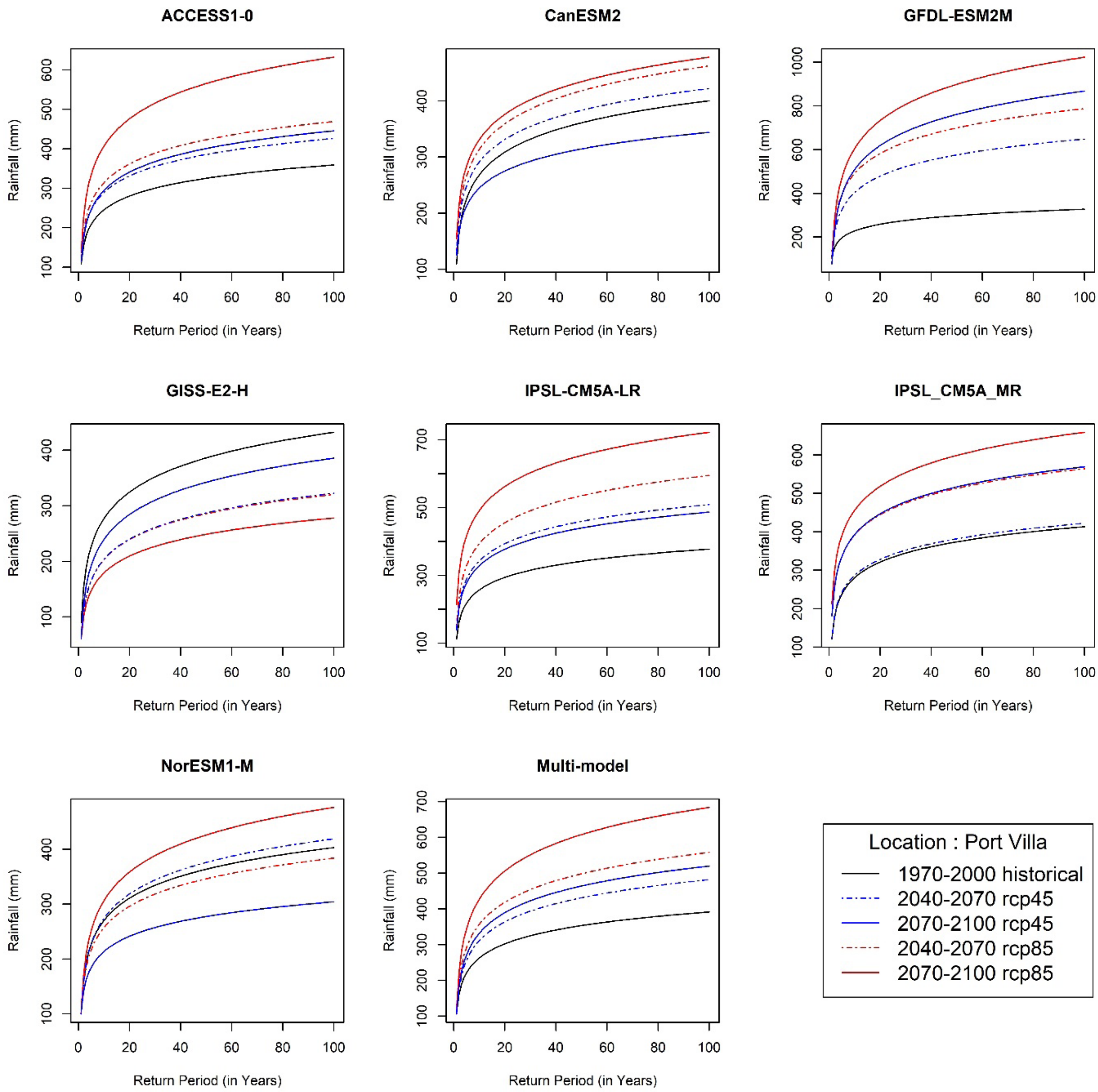

Figure 7: Average recurrence interval (ARI) curves of yearly maximum rainfall for Port Vila (168.32 E, 17.74 S) using the Gumbel extreme value distribution. Comparison with historical 1970 – 2000 (black), RCP 4.5 2040 – 2070 (blue dashed) RCP 4.5 2070 – 2100 (blue), RCP 8.5 2040 – 2070 (red dashed) and RCP 8.5 2070 -2100 (red) has been shown for seven climate models and the multi-model average. The multi-model mean indicates an increase in extreme rainfall intensity for a given return period.

2. Tropical cyclones

Tropical cyclone data

The observational tropical cyclone (TC) data were sourced from the South Pacific Enhanced Archive of Tropical Cyclones database (SPEArTC) (Diamond et al., 2012), where the best track data are mostly available at 6-hour intervals for the entire TC lifecycle. The wind speed for each TC is the maximum 10-minute sustained wind speed in knots (Diamond et al., 2012) that was converted to m/s using the conversion 1 knot = 0.51 m/s. Cyclones were also categorised according to the conventional definition of Southern Hemisphere TC season, i.e., from 1st July to 30th June of the following year, with the following year representing a particular TC season, e.g. 1 July 2022 to 30 June 2023 is defined as the 2023 TC season.

The modelled TC data were obtained from Chand et al. (2017) and Bell et al. (2019), where they used a suite of climate models from the Coupled Model Intercomparison Project phase 5 (CMIP5) dataset (Taylor et al., 2012) to simulate TCs using the Okubo-Weiss-Zeta (OWZ) detection and tracking scheme (Tory et al., 2013a; Tory et al., 2013b). Both studies evaluated two scenarios: (1) the current-climate simulation (1970–2000) and (2) the future-climate simulation (2070–2100) under a high emissions pathway (RCP8.5). These datasets also included 850-hPa wind speeds that were converted to surface winds using a conversion factor of 0.8 (Franklin et al., 2003). We evaluated simulated TC tracks from 13 models (Table 5) for both historical and future scenarios.

Table 5: List of 13 CMIP5 models used for TC wind speed analysis along with time periods for the historical and future (RCP8.5) scenarios, based on data availability.

Models	Historical period	RCP8.5 period
SPEArTC	1970–2000	
ACCESS1.0	1970–2000	2070–2100
ACCESS1.3	1970–2000	2070–2100
BCC-CSM1.1	1970-2000	2069–2099
BCC-CSM1.1M	1970–2000	2070–2100
CCSM4	1970–2000	2070–2100
CNRM-CM5	1970–2000	2070–2100
CSIRO-MK3.6	1970–2000	2070–2100
GFDL-CM3	1970–2000	2070–2100
GFDL-ESM2G	1970–2000	2070–2100
GFDL-ESM2M	1970–2000	2070–2100
HadGEM2-ES	1970–2000	2069–2099
MIROC5	1970–2000	2070–2100
MRI_CGCM3	1970–2000	2070–2100

Data mining and quality control

Three buffer regions (Figure 8) were created (50 km, 250 km and 500 km) around all of Vanuatu, followed by a 500 km buffer around each province. These three buffers were used to extract TC tracks from all three datasets (i.e., SPEArTC, 13 historical simulations and 13 RCP8.5 simulations) for the whole Vanuatu region, as well as for each province using the 500 km buffer. The extracted data were then quality-checked, ensuring that all TC track points (6-hour timestep for SPEArTC and 12-hour for CMIP5 models) within each buffer were extracted. For cases where a TC track traversed the buffer region but without a 6-hour (for SPEArTC) or 12-hour (for climate models) timestep, a timestep was estimated (especially for the 850-hPa TC wind speed) via a simple interpolation.

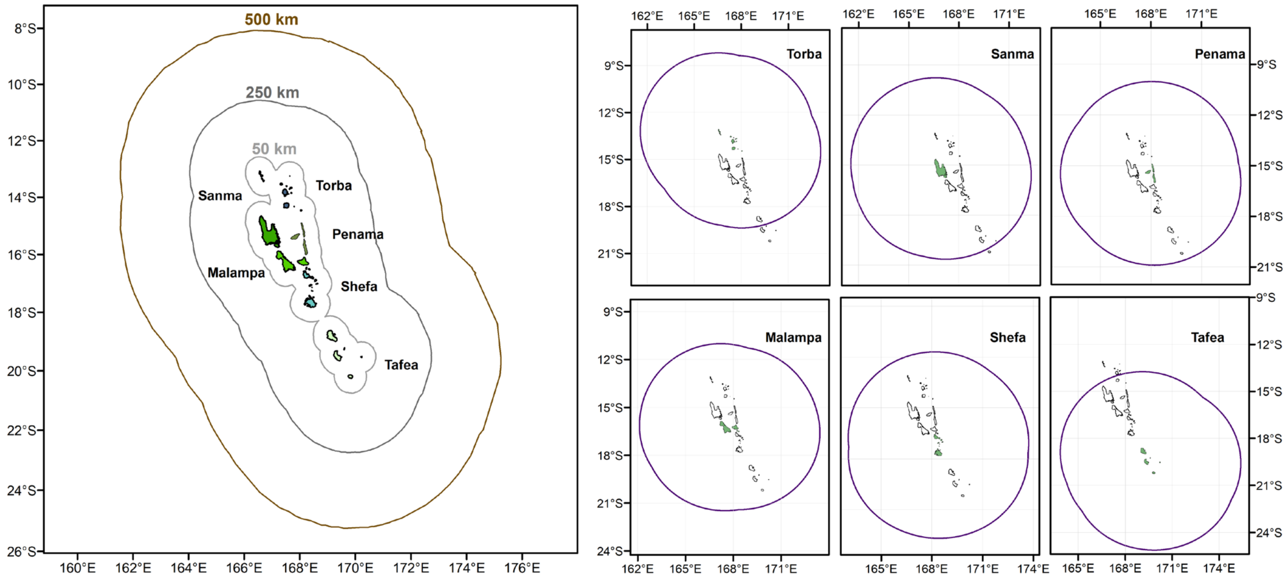

Figure 8: (Panel a) Map of Vanuatu along with the three buffers (50 km, 250 km and 500 km) used to extract TC tracks. Panel b shows a 500 km buffer around each province.

Statistical calibration

The TC wind speeds extracted from the climate models were calibrated so that the reconstructed data resembled the observed data as closely as possible. This was achieved using quantile matching with the help of a cubic spline approach, as discussed above. The 13 CMIP5 climate models (Table 6) for historical and RCP8.5 scenarios were calibrated with respect to the observational data (SPEArTC) (Figure 9). A bin size of 10 was determined using the Root Mean Square Estimate (RMSE) (Biswas et al., 2022).

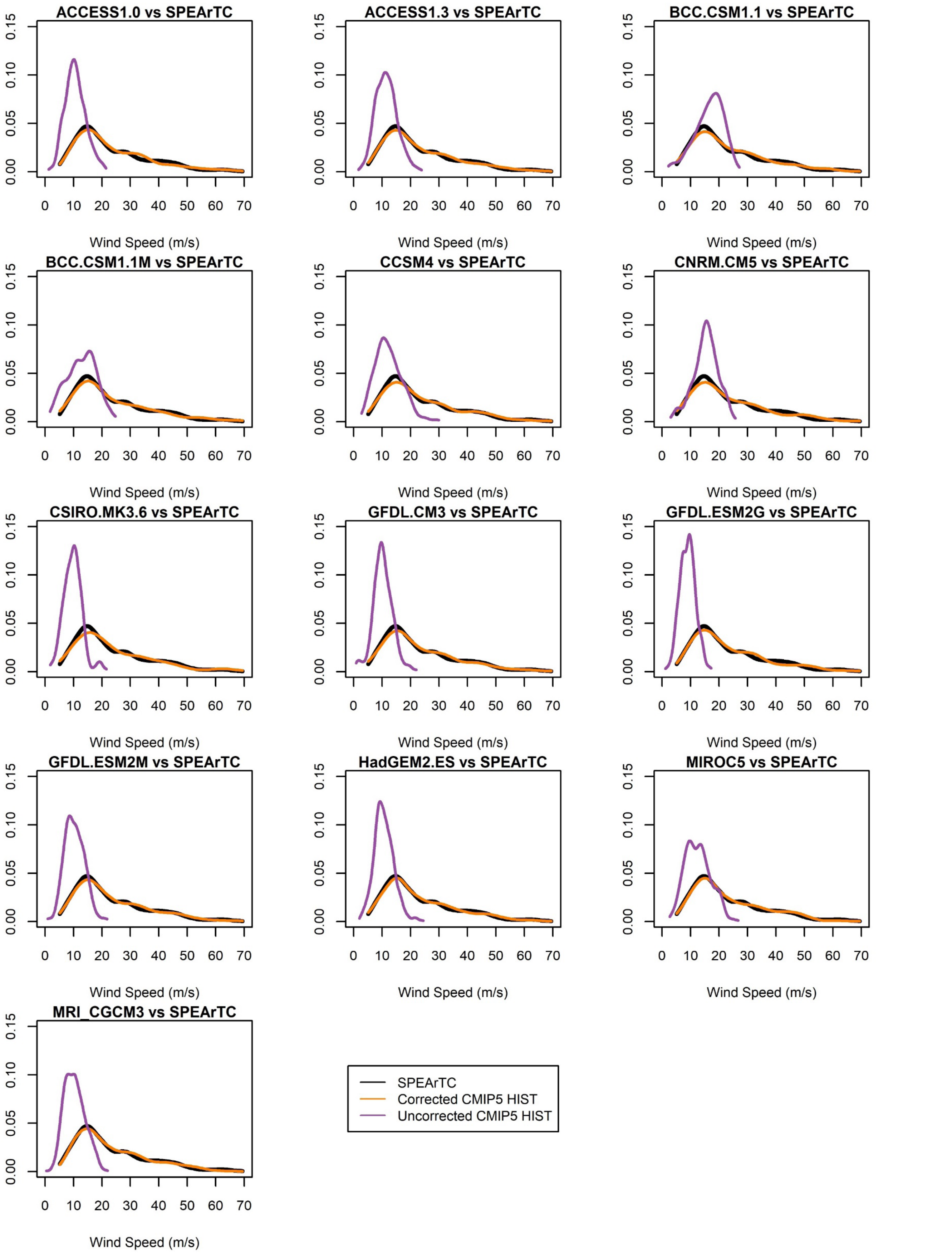

Figure 9: Kernel density graphs of TC wind speed data for 1970-2000 (within the 500 km buffer) using the cubic spline method. Each graph illustrates the observed data (SPEArTC in black), uncorrected CMIP5 data (purple) and bias-corrected model data (orange). A close match between the SPEArTC data and corrected CMIP5 data indicates that the calibration method is performing well.

Temporal analyses

The calibrations applied to the historical climate model data were also applied to the future climate model data. This bias-corrected dataset was then used to collate TC intensity information for each province, followed by a quality check, as mentioned above. TCs with wind speed reaching 17.5 m/s during 1970–2000 (representing the late 20th century) and 2070–2100 (late 21st century) were considered for further analyses. For two models, BCC-CSM1.1 and HadGEM2-ES, their late 21st century period is 2069–2099 (see Table 5).

An additional step was taken to identify the best-performing models because Bell et al. (2019) highlighted some caveats associated with the outputs from the OWZ TC detector. Their study showed that the TC detection scheme sometimes tends to underestimate or overestimate TC frequency, potentially impacting the projection assessments. Bell et al. (2019) objectively defined specific measures to eliminate errors and achieve a more accurate climatology. We used one such definition: the number of simulated TCs should be within ± 50% of the TC counts in SPEArTC (i.e., the observed climatology). Using this criterion, eight best-performing models were selected for all analyses in this study (Table 6). These eight models were also identified as the best-performing models by Chand et al. (2017).

Table 6: Total number of TCs extracted within each buffer for all 13 CMIP5 models (both historical and RCP8.5). The bold TC numbers indicate the best-performing models that simulated at least 50% of total observed TCs from SPEArTC.

CLIMATE MODELS	HISTORICAL TCS			RCP8.5 TCS		
	500 km	250 km	50 km	500 km	250 km	50 km
SPEArTC	105	73	40			
ACCESS1.0	69	51	27	73	49	27
ACCESS1.3	82	57	33	124	90	46
BCC-CSM1.1	51*	24*	14*	42	24	12
BCC-CSM1.1M	41	24	8	49	26	9
CCSM4	41	35	19	32	22	13
CNRM-CM5	27	18	10	17	10	4
CSIRO-MK3.6	32	19	11	73	48	33
GFDL-CM3	42	30	20	31	17	4
GFDL-ESM2G	57	34*	10*	41	24	10
GFDL-ESM2M	59	36*	17*	44	23	9
HadGEM2-ES	80	53	32	55	31	14
MIROC5	89	52	29	53	33	16
MRI-CGCM3	109	65	42	91	63	41

* Even though this model's climatology is not within ±50% of SPEArTC, either/or it's very close, and has been identified as a best performing model by Chand et al. (2017); hence, it was included for further analyses.

For all analyses, we used the maximum TC wind speed along the TC track within the buffer as our emphasis is on extremes. We evaluated the TC climatology as per the observational data (time-series for the 1971–2021 TC season) at the national and provincial levels. Projected changes in TC intensity and frequency from the selected models were assessed in two ways (both at national and provincial levels): firstly, by evaluating "All TCs" (from categories 1 to 5) and secondly, only considering "Severe TCs" (categories 3 to 5). TCs were sorted into respective categories using the Australian TC intensity scale (Table 7). In both cases, TC intensities and TC frequencies were analysed between the current and future climate conditions. Consequently, projected changes in these TC metrics (frequency and intensity) were derived by computing their percentage changes. The Gumbel function was used to construct ARIs. We also combined the eight models to form a multi-model average and performed similar analyses.

Table 7: TC classification is based on the Australia/Fiji intensity scale. Maximum wind refers to the 10-minute sustained windspeed.

Category	Maximum wind (km/hr)
1	63 – 88
2	89 – 117
3	118 – 159
4	160 – 200
5	> 200

Projected changes in TC frequency and intensity

The projected changes in TC frequency and TC intensity are shown in Figure 10 for the two provinces. Out of eight models, six and seven models demonstrate a projected decrease in TC frequency in the future climate for Shefa and Sanma provinces, respectively (Figure 10, left panel). Conversely, TC intensities are projected to increase at both locations, indicated by seven (for Shefa) and six (for Sanma) models (Figure 10, right panel).

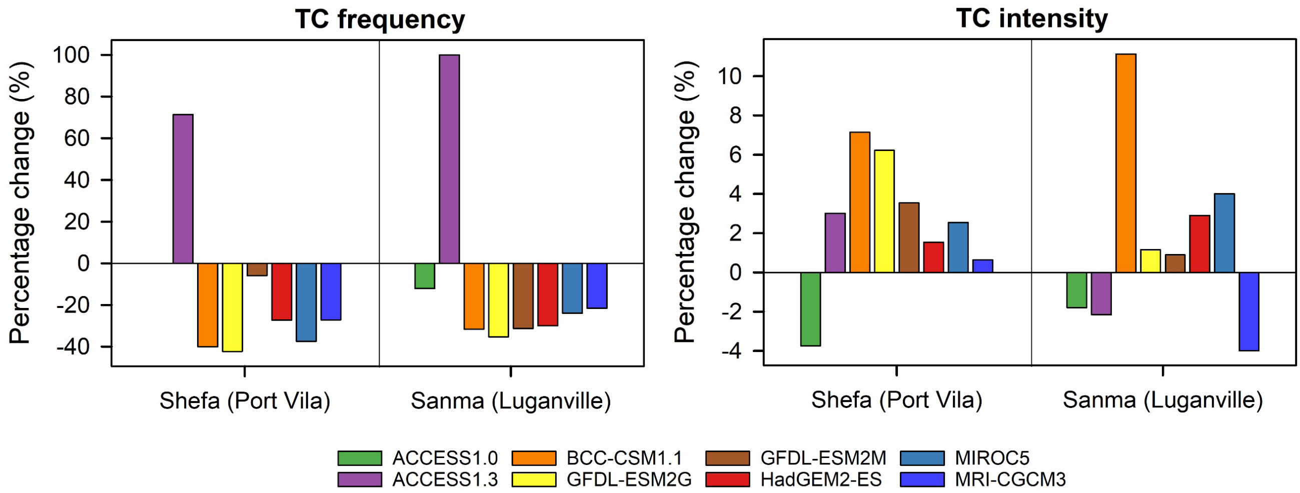

Figure 10: Percentage change in mean TC frequency (left panel) and TC intensity (right panel) between the current and future climate conditions for the eight CMIP5 models. These projections are for Shefa (city: Port Vila) and Sanma (city: Luganville) provinces (labelled on horizontal axes). Most models indicate a decline in TC frequency and an increase in TC intensity in the future climate for both cities.

Intensity-frequency curves

Two example curves for TC intensity-frequency changes between historical and future periods are shown below for two provinces: Shefa (which includes Port Vila; Figure 11) and Sanma (which includes Luganville; Figure 12). Most models simulate an increase in extreme windspeeds. The multi-model average for Shefa indicates that the increase is about 6% for all return periods (Figure 13, top row). The multi-model average for Sanma indicates that the increase is about 3% for all return periods (Figure 13, bottom row).

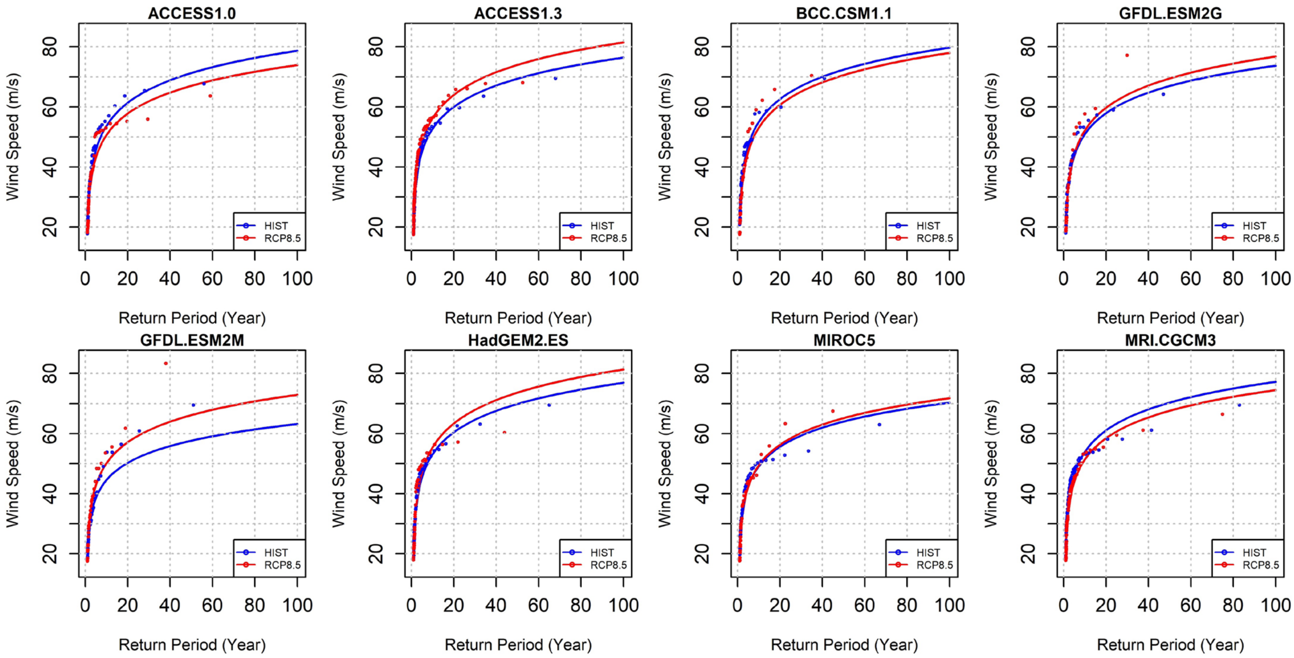

Figure 11: Average intensity-frequency curves of maximum TC wind speed intensity for Shefa province (city: Port Vila). Comparisons are for historical 1970 – 2000 (blue) and RCP 8.5 2070 – 2100 (red) cases. Five out of eight models simulate an increase in extreme windspeed.

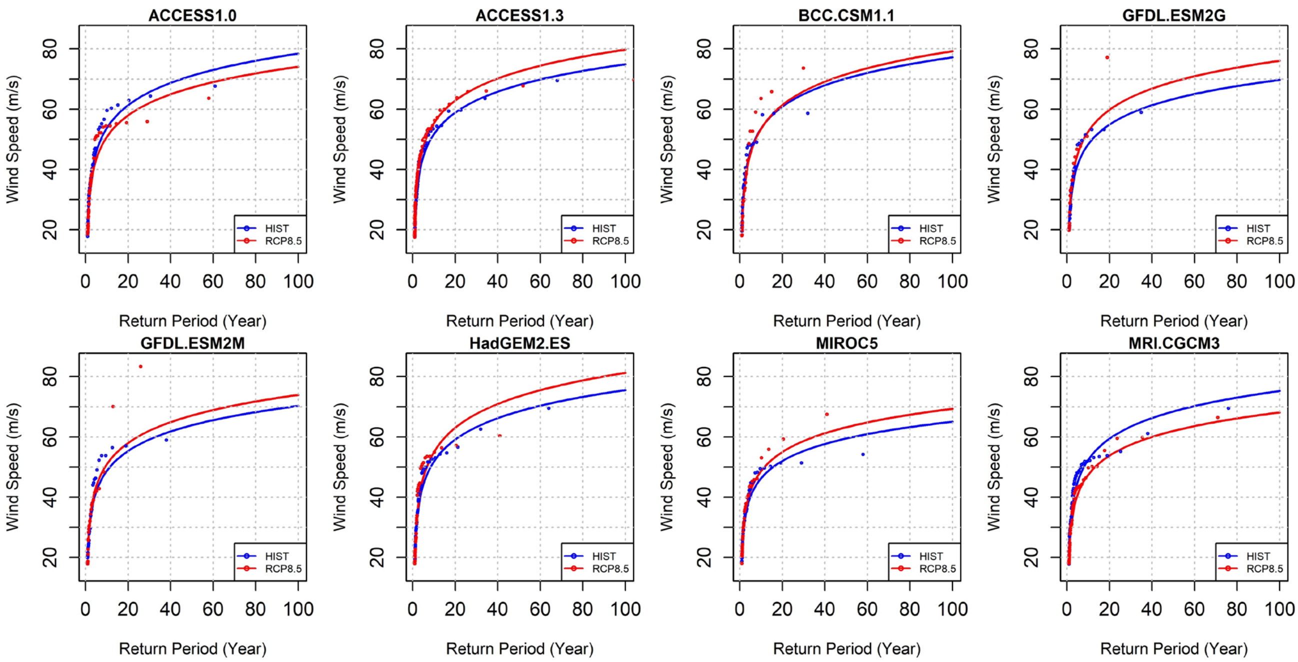

Figure 12: As in Figure 11, but for Sanma Province (city: Luganville). Six out of eight models simulate an increase in extreme wind speed.

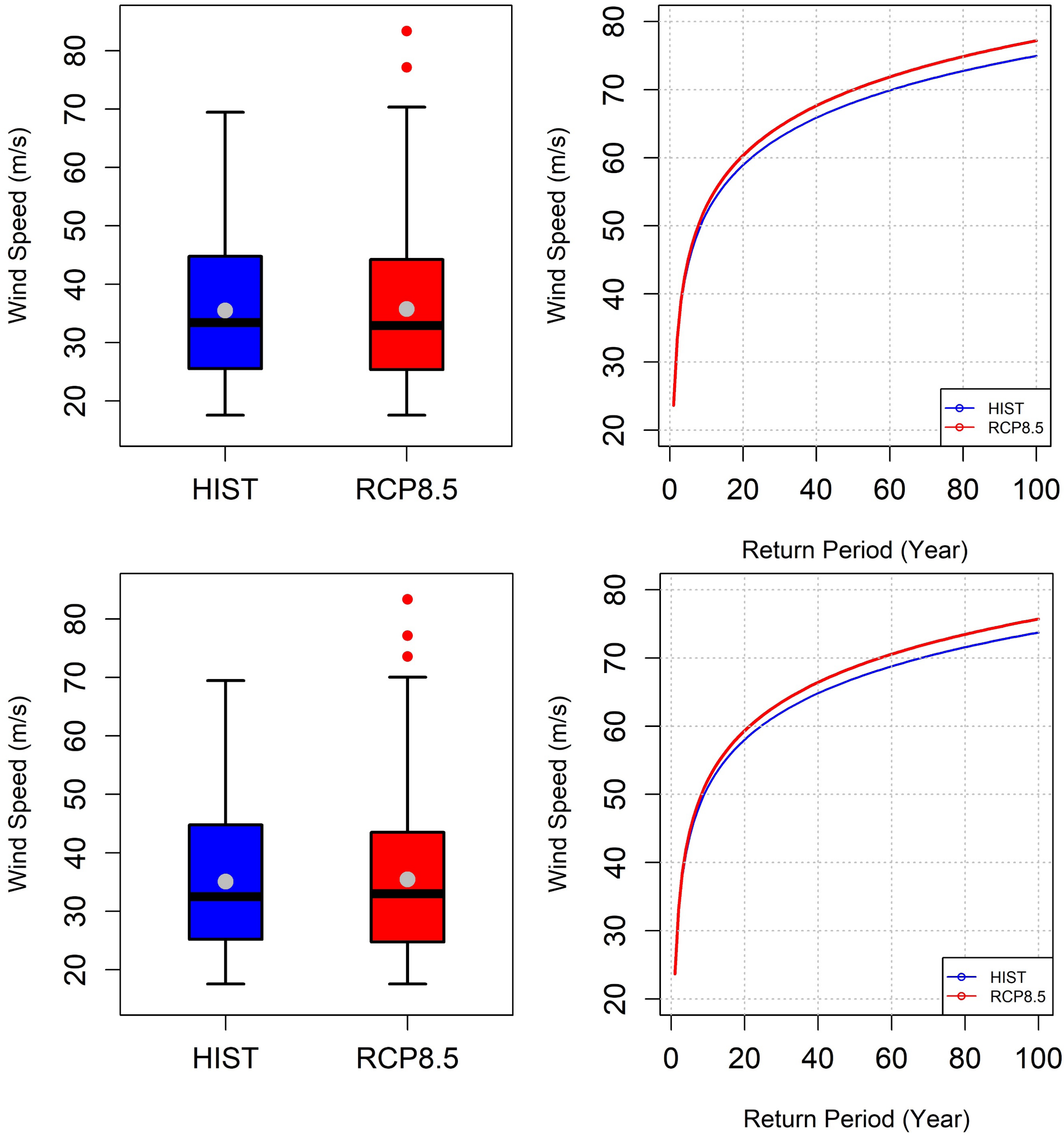

Figure 13: TC wind speed distribution (left) and ARIs (right) of all eight models combined to form a multi-model average for Shefa (city: Port Vila; top row) and Sanma (city: Luganville; bottom row) provinces. The multi-model average at both locations shows an increase in extreme wind speed.

Discussion

In this study, we assessed projected changes in extreme rainfall and windspeed for Vanuatu.

We have used ARI curves to show the projected change in annual maximum daily rainfall for 2040-2070 and 2070-2100 for low and high emission scenarios. A general increase in extreme rainfall intensity is simulated for both Port Vila and Luganville. There are some differences in ARI curves between climate models. For example, GISS-E2-H shows a decrease in extreme rainfall intensities at Port Villa while CanESM2 shows a decrease at Luganville. So, the return period values should be interpreted with caution. The extreme rainfall data can be used in current and future flood risk assessments. New Zealand NIWA is undertaking an ADB-sponsored flood risk assessment for Luganville that incorporates our extreme rainfall projections and overlays an exposure database that includes buildings and infrastructure. This will inform adaptation planning.

We also used ARI curves to assess projected changes in TC windspeeds. Assessing the vulnerability of a specific region to TCs is an essential step in formulating enhanced strategies for disaster preparedness. We investigated the potential impact of anthropogenic greenhouse warming on the frequency and intensity of TCs, specifically for the Vanuatu region (including all six provinces).

Overall, the projections indicated a decline in TC frequencies; however, TCs will likely have enhanced intensities in the future scenario relative to the current climate – consistent with previous findings (Tory et al., 2013; Walsh et al., 2016; Chand et al., 2017; Bell et al., 2019; Knutson et al., 2020; CSIRO and SPREP, 2021). Projections derived from the other two buffers (i.e., 250 km and 50 km) revealed consistent trends, adding more lines of evidence to support our findings. It is worth mentioning that the consensus found in these other studies was generally for the broader South Pacific area. However, our findings offer additional evidence concerning the projections of both frequency and intensity of TCs for Vanuatu, and all its six provinces, exclusively.

The results from provincial analyses were insightful, given that they demonstrated the hazards different regions are likely to encounter due to TCs when approaching the end of the 21st century. For instance, the 6% increase in intensity derived at Port Vila (within Shefa province in central Vanuatu) is larger than the 3% increase at Luganville (northwestern side within Sanma province).

The information gained from these projections is important regarding adaptation and planning. Port Vila and Luganville are the most populous areas with the largest number of buildings and infrastructure, thus incurring the greatest loss and damage from TCs, including critical infrastructure, disruption of livelihoods, threats to water and food security, compromising health and affecting education. One study estimated that 5145 buildings in Luganville and 2115 buildings in Port Vila are at risk of heavy damage from an extreme wind event with a 100-year return period (Beca, GNS and NIWA, 2016). UN.ESCAP (2021) has indicated that Vanuatu's expenses (approx. USD 1.1 billion) sustained from natural disasters could increase to USD 1.4 billion in a worst-case scenario (RCP8.5), which can risk the country losing about 20% of its annual gross domestic product. Hence, relevant agencies (e.g., Meteorological Services, National Disaster Management Offices and Departments of Climate Change) must utilise this information efficiently to enhance the adaptation and planning process. It is also crucial that this information is clearly communicated to sector stakeholders and the wider community through their information products and awareness programmes.

Conclusions

Extreme daily rainfall is expected to increase in future due to climate change. Historical weather station data, reanalysis data, seven climate model simulations and extreme value analysis were combined to estimate current and future extreme rainfall for Port Vila and Luganville. The current baseline was defined as 1970-2000, while the future periods were 2040-2070 and 2070-2100. Low (RCP4.5) and high (RCP8.5) greenhouse gas emissions scenarios were considered. For extreme daily rainfall with return periods of 10-100 years, the multi-model mean results for Port Vila showed an increase of about 21% for 2040-2070 RCP4.5, 30% for 2070-2100 RCP4.5, 40% for 2040-2070 RCP8.5 and 70% for 2070-2100 RCP8.5. For return periods of 10-100 years, the multi-model mean results for Luganville showed an increase of about 18% for 2040-2070 RCP4.5, 27% for 2070-2100 RCP4.5, 26% for 2040-2070 RCP8.5 and 57% for 2070-2100 RCP8.5. These increases have significant implications for future flood risk management strategies.

Although Vanuatu is experienced in responding to cyclones, a double event such as TC Judy and TC Kevin in March 2023 presented unprecedented challenges. Tropical cyclones are projected to become less frequent in future, but the average intensity is projected to increase. Therefore, developing a more comprehensive understanding of cyclone behaviour is essential to inform adaptation strategies across different sectors. Such understanding can also enhance the general public's resilience to the destructive impacts of extreme events, particularly in a worst-case scenario. Reanalysis data, eight climate model simulations and extreme value analysis were combined to estimate current and future extreme windspeeds for Port Vila and Luganville. The current baseline was defined as 1970-2000, while the future period was 2070-2100. A high (RCP8.5) greenhouse gas emissions scenario was considered. For extreme TC windspeed with return periods of 10-100 years, the multi-model mean results showed an increase in the intensity of about 6% for Port Vila and 3% for Luganville. These increases have implications for future cyclone risk management strategies.

Additionally, decision-makers such as environmental managers and city planners can use these projections along with suitable exposure and vulnerability to undertake detailed risk assessments in Vanuatu. This can facilitate more effective adaptation strategies across various sectors, complementing previous findings (e.g., Beca, GNS and NIWA, 2016).

References

Beca, GNS and NIWA (2016). Urban Risk Assessment and Geo-data Management Report: Risk Mapping and Planning for Urban Preparedness (Contract No. C.06). Prepared for Vanuatu Meteorological and Geo-hazards Department by Beca International Consultants Ltd (Beca), GNS Science and the National Institute of Water and Atmospheric Research (NIWA), 228 pages.

Bell SS, Chand SS, Camargo SJ, Tory KJ, Turville C, Ye H (2019) Western North Pacific Tropical Cyclone Tracks in CMIP5 Models: Statistical Assessment Using a Model-Independent Detection and Tracking Scheme. Journal of Climate 32:7191-7208. https://doi.org/https://doi.org/10.1175/JCLI-D-18-0785.1.

Biswas S, Chand SS, Dowdy AJ, Wright W, Foale C, Zhao X, Deo A (2022) Statistical Calibration of Long-Term Reanalysis Data for Australian Fire Weather Conditions. Journal of Applied Meteorology and Climatology 61:729-758. https://doi.org/10.1175/jamc-d-21-0034.1.

Chand SS, Tory KJ, Ye H, Walsh KJE (2017) Projected increase in El Niño-driven tropical cyclone frequency in the Pacific. Nature Climate Change 7:123-127. https://doi.org/10.1038/nclimate3181.

CSIRO and SPREP. (2022). Tropical Cyclones and Climate Change : implications for the Western Tropical Pacific. https://doi.org/https://doi.org/10.25919/pbtc-1y82

CSIRO, & SPREP. (2021). “NextGen” Projections for the Western Tropical Pacific: Current and Future Climate for Vanuatu. https://doi.org/https://doi.org/10.25919/hexz-1r10

Diamond HJ, Lorrey AM, Knapp KR, Levinson DH (2012) Development of an enhanced tropical cyclone tracks database for the southwest Pacific from 1840 to 2010. International Journal of Climatology 32:2240-2250. https://doi.org/https://doi.org/10.1002/joc.2412.

Doblas-Reyes FJ, Pavan V, Stephenson DB (2003) The skill of multi-model seasonal forecasts of the wintertime North Atlantic Oscillation. Climate Dynamics 21:501-514. https://doi.org/10.1007/s00382-003-0350-4.

Donat MG, Leckebusch GC, Wild S, Ulbrich U (2010) Benefits and limitations of regional multi-model ensembles for storm loss estimations. Climate Research 44:211-225, https://www.int-res.com/abstracts/cr/v44/n2-3/p211-225/.

Franklin JL, Black ML, Valde K (2003) GPS Dropwindsonde Wind Profiles in Hurricanes and Their Operational Implications. Weather and Forecasting 18:32-44. https://doi.org/https://doi.org/10.1175/1520-0434(2003)018<0032:GDWPIH>2.0.CO;2.

Knutson, T., Camargo, S. J., Chan, J. C. L., Emanuel, K., Ho, C. H., Kossin, J., Mohapatra, M., Satoh, M., Sugi, M., Walsh, K., & Wu, L. (2020). Tropical cyclones and climate change assessment. Bulletin of the American Meteorological Society, 100(10), 1987–2007. https://doi.org/10.1175/BAMS-D-18-0189.1

Li J, Heap AD (2014) Spatial interpolation methods applied in the environmental sciences: A review. Environmental Modelling & Software 53:173-189. https://doi.org/10.1016/j.envsoft.2013.12.008.

Moss RH, Edmonds JA, Hibbard KA, Manning MR, Rose SK, van Vuuren DP, Carter TR, Emori S, Kainuma M, Kram T, Meehl GA, Mitchell JFB, Nakicenovic N, Riahi K, Smith SJ, Stouffer RJ, Thomson AM, Weyant JP, Wilbanks TJ (2010) The next generation of scenarios for climate change research and assessment. Nature 463:747-756. https://doi.org/10.1038/nature08823.

Mudashiru RB, Abustan I, Sabtu N, Mukhtar HB, Balogun W (2023) Choosing the best fit probability distribution in rainfall design analysis for Pulau Pinang, Malaysia. Modeling Earth Systems and Environment. https://doi.org/10.1007/s40808-022-01668-0.

Petrou M, Petrou C (2010) Image Restoration. Image Processing: The Fundamentals. pp 395-526.

Piani C, Weedon GP, Best MJ, Gomes SM, Viterbo PA, Hagemann S, Haerter JO (2010) Statistical bias correction of global simulated daily precipitation and temperature for the application of hydrological models. Journal of Hydrology 395:199-215. https://doi.org/10.1016/j.jhydrol.2010.10.024.

Sheather SJ, Jones MC (1991) A Reliable Data-Based Bandwidth Selection Method for Kernel Density Estimation. Journal of the Royal Statistical Society Series B (Methodological) 53:683-690, http://www.jstor.org/stable/2345597.

Silverman B (1986) Density Estimation for Statistics and Data Analysis. Chapman and Hall, London.

Taylor KE, Stouffer RJ, Meehl GA (2012) An Overview of CMIP5 and the Experiment Design. Bulletin of the American Meteorological Society 93:485-498. https://doi.org/10.1175/bams-d-11-00094.1.

Teutschbein C, Seibert J (2012) Bias correction of regional climate model simulations for hydrological climate-change impact studies: Review and evaluation of different methods. Journal of Hydrology 456-457:12-29. https://doi.org/10.1016/j.jhydrol.2012.05.052.

Tory KJ, Chand SS, Dare RA, McBride JL (2013a) The Development and Assessment of a Model-, Grid-, and Basin-Independent Tropical Cyclone Detection Scheme. Journal of Climate 26:5493-5507. https://doi.org/https://doi.org/10.1175/JCLI-D-12-00510.1.

Tory KJ, Dare RA, Davidson NE, McBride JL, Chand SS (2013b) The importance of low-deformation vorticity in tropical cyclone formation. Atmos Chem Phys 13:2115-2132. https://doi.org/10.5194/acp-13-2115-2013.

Tory, K. J., Chand, S. S., McBride, J. L., Ye, H., & Dare, R. A. (2013). Projected Changes in Late-Twenty-First-Century Tropical Cyclone Frequency in 13 Coupled Climate Models from Phase 5 of the Coupled Model Intercomparison Project. Journal of Climate, 26(24), 9946–9959. https://doi.org/10.1175/JCLI-D-13-00010.1

UN.ESCAP. (2021). Resilience in a riskier world : managing systemic risks from biological and other natural hazards. In Asia Pacific Disaster Report 2021. https://hdl.handle.net/20.500.12870/3811

van Vuuren DP, Edmonds J, Kainuma M, Riahi K, Thomson A, Hibbard K, Hurtt GC, Kram T, Krey V, Lamarque J-F, Masui T, Meinshausen M, Nakicenovic N, Smith SJ, Rose SK (2011) The representative concentration pathways: an overview. Climatic Change 109:5. https://doi.org/10.1007/s10584-011-0148-z.

Walsh, K. J. E. E., Mcbride, J. L., Klotzbach, P. J., Balachandran, S., Camargo, S. J., Holland, G., Knutson, T. R., Kossin, J. P., Lee, T. cheung, Sobel, A., & Sugi, M. (2016). Tropical cyclones and climate change. Wiley Interdisciplinary Reviews: Climate Change, 7(1), 65–89. https://doi.org/doi:10.1002/wcc.371

Wolf PR, Dewitt BA, Wilkinson BE (2014) Digital Resampling. Fourth edition. edn. McGraw-Hill Education, New York

SPREP 2023